


EDITED BY
DOUGLAS H. WERNER AND ZHI HAO JIANG

Electromagnetics of Body Area Networks

Antennas, Propagation, and RF Systems




IEEE PRESS

WILEY

More than Wearable: Epidermal Antennas for Tracking and Sensing

S. Amendola, C. Occhiuzzi, G. Marrocco

1. INTRODUCTION	3
2. RFID TECHNOLOGY	4
3. RADIATION PERFORMANCE OF EPIDERMAL ANTENNAS	7
3.1 Efficiency and gain vs. antenna size	8
3.2 Gain vs. the trace width	9
3.3 Radiation performance vs. the trace conductivity	10
3.4 Radiation performance vs. the spacing from the skin	11
4. PERFORMANCE OF EPIDERMAL RFID DUAL LOOP-TAG	13
4.1 Tag Layout	13
4.2 Prototype and on-skin Performance	14
4.3 On-skin retuning	17
4.3.1 Examples	19
5. SPECIAL (FUNCTIONALIZED) EPIDERMAL MEMBRANES	21
5.1 Scaffold membranes: Poli(ϵ -caprolactone)	21
5.2 Hydrogel membranes	23
6. SENSING APPLICATIONS	25
6.1 Epidermal RF Thermometer	25
6.2 Smart-plaster for wound healing	28
6.2.1 Idea	28
6.2.2 Prototype and test	29
7. SUMMARY AND CONCLUSIONS	31
8. REFERENCES	34

Error! Bookmark not defined.

1. Introduction

Epidermal or *Skin Electronics* [1] is a currently emerging research trend combining multi-disciplinary backgrounds such as Material science, Mechanics, classic Electronics and Electromagnetics, and Communications. Recently published works [2], demonstrate the possibility to fabricate skin-like electronics and sensors that are suitable to be deployed over thin and bio-compatible conformable membranes for direct placement over living organisms (e.g. tissues), environmental substrates (plants or stems), and foods [3]. The direct “on-skin” sampling of surface temperature, humidity, pH, deformations, skin impedance, and electrophysiological potentials by means of plaster-like complex devices may enable a host of new applications to consumer electronics, human health and wellness as well as to nutrition.

Most of the scientific efforts presented so far have been oriented to high-tech fabrication methods for epidermal devices (spin-coating, photolithography, dry etching, and transfer printing) e.g. to the design of engineered thin, lightweight, stretchable conformal silicone and polyvinyl alcohol (PVA) substrates as well as to the deposition of conducting traces. Most of the described prototypes relied on wired interconnection for data transfer [4] or, at most, by inductive coupling among coils [5],[6] that permit only near-contacting links.

In this scenario, the virtuous synergy of Epidermal Electronics with the well-assessed passive Radiofrequency Identification (RFID) technology [7] could boost the usability of skin devices in the real world, providing a further brick of the quickly emerging Internet of Things [8]. The communication through electromagnetic backscattering, as involved in the RFID architectures, requires just a small battery-less IC transponder that is fully compatible with thin and flexible devices. Furthermore, thanks to the intrinsic sensing capabilities of RFID platforms [9], it could be possible to exploit the simple interaction between the tag and the skin to retrieve data and information about the state of the human body without the need of dedicated and complex electronics integrated into the epidermal device. However, the cohabitation of passive antenna elements with the human skin, or with living matters in general, represents an intrinsic challenge due to the high losses of tissues which strongly degrade the radiation efficiency of the device and accordingly the length of the communication link. This problem has been widely addressed by the research on wearable antennas wherein the goal is however to decouple at most the antenna radiation from the body loss by means of ground planes (patch-like antennas) [10][11] or multi-layer spacers placed between the body and a dipole [12], a slot [13], or a loop antenna [14]. Conversely, an RFID tag for epidermal applications has to act as both an antenna and as a sensor therefore, unlike wearable tags, it has to be placed in direct contact with the body. Very thin insulating materials need to be used, mostly

acting as an adhesive interface between the conductor/electronics and the skin. The epidermal tag has moreover to be designed in order not to interfere with the local metabolism of the skin. Accordingly, the substrate is required to be not only bio-compatible but also breathable (in order not to perturb the transpiration and the local temperature of the skin). Shielding planes, as in the case of patch antennas, have to be avoided, and the amount of antenna conductor has to be minimized.

Some early and pioneering examples of epidermal antennas, in the form of shaped dipoles, have been very recently proposed in [15], [16], and [17] and consider temporary tattoo-like RFID tags. Conductive paints, profiled by stencils and inkjet printing, were used to fabricate the antenna element for the direct application over the skin and over the tongue to detect the motion of impaired people. The reported read distances are of the order of 1m. The performance of several types of thin single-layer antennas (e.g. slot, self-complementary and wire antenna) for plaster-like sensing applications at 2.4 GHz were extensively investigated in [18] to search for the antenna layout that was best suited to operate in the very close proximity of the human body.

This chapter introduces the performance, the natural bounds, and some possible applications to bodycentric systems of epidermal antennas that are suitable to be integrated with RFID technology. Starting from basic principles, the maximum efficiency and gain are related to the geometrical and electrical parameters of the epidermal device. Then a reference antenna layout is extensively used to discuss the issues arising from the placement of the antenna over different parts of the body and to introduce a practical on-body impedance retuning mechanism. Specialized membranes useful to host epidermal antennas and to achieve sensing capabilities are introduced as well.

The chapter ends with the description of two promising applications of epidermal tags to the wireless measurement of body temperature and to the monitoring of fluid exchanges at the skin interface.

2. RFID technology

An RFID system [7] is comprised of two main components: the remote transponder or tag, including an antenna and a microchip transmitter, located on the object to be identified, and the local querying system or reader which can collect the data transmitted from the tag and eventually perform a preliminary processing job. Various kinds of data and, first of all, a unique identification code (ID), can be wirelessly transferred to the reader by means of radio-frequency electromagnetic signals.

The tags could be *passive*, harvesting energy from the interrogating system, *semi-active* when a battery is included only to feed embedded sensors or to increase the

sensitivity of the receiver inside the microchip, or *fully active* where a local source directly feeds a microcontroller as well as the transmitting radio. Battery-less tags have an almost unlimited life, are very low cost, lightweight and need no maintenance. Because of the absence of a local power source, passive transponders provide the greatest flexibility to seamlessly integrate the RF devices with the human skin as required by epidermal applications.

RFID systems can be classified in terms of operating frequencies: LF (Low Frequency, 120-145 KHz), HF (High Frequency, 13.56 MHz), UHF (Ultra High Frequency, 866-956 MHz). UHF devices, although strongly influenced by high dielectric targets, as in the case of the human body, may in principle promise larger activation ranges which enable a real ease of interrogation of epidermal tags thus making the UHF-RFID standard particularly attractive over the HF frequency.

This chapter is hence focused only on passive battery-less UHF systems.

The power budget of the UHF-RFID radio channel, i.e. the power $P_{R \rightarrow T}$ transmitted by the reader and collected by the tag (direct link), and the power $P_{R \leftarrow T}$ backscattered by the tag towards the reader (backward link), are commonly characterized in far field by means the Friis formula and the radar equation [7]:

$$P_{R \rightarrow T} = \left(\frac{\lambda_0}{4\pi d} \right)^2 P_{in} G_R G_{Tag} \tau \cdot \eta_P \quad (1)$$

$$P_{R \leftarrow T} = \frac{1}{4\pi} \left(\frac{\lambda_0}{4\pi d^2} \right)^2 P_{in} G_R^2 r_{CS_T} \eta_P \quad (2)$$

where $\hat{G}_{Tag} = G_{Tag} \cdot \tau$ is the realized gain of the tag, i.e. the radiation gain G_{Tag} of the tag antenna reduced by the power transfer coefficient τ between tag antenna and the microchip, P_{in} is the power emitted by the reader, G_R is the reader antenna gain, η_P is the polarization factor between the reader and the tag, d is the distance between reader and tag antennas, λ_0 is the free-space wavelength, and r_{CS_T} is the Radar Cross Section of the tag.

The power transmission coefficient, can be expressed in terms of tag antenna and tag IC impedance $Z_A = R_A + iX_A$ and $Z_{chip} = R_{chip} + iX_{chip}$ by

$$\tau = \frac{4R_{chip}R_A}{|Z_{chip} + Z_A|^2} < 1 \quad (3)$$

The performance indicator of an on-body tag for reliable indoor monitoring is the maximum reading range d_{max} between reader and tag. The read range is dependent on the antenna radiation characteristics of the antenna (\hat{G}_{Tag}) and

inversely dependent on the IC sensitivity (P_{chip}), e.g. the power required to activate the IC. The maximum theoretical read range can be estimated from (1) as:

$$d_{\text{max}} = \left(\frac{\lambda_0}{4\pi} \right) \sqrt{\frac{\text{EIRP} \cdot \hat{G}_{\text{Tag}} \cdot \eta_P}{P_{\text{chip}}}} \quad (4)$$

where $\text{EIRP} = G_R \cdot P_{\text{in}}$ is the Equivalent Isotropic Radiated Power emitted by the reader and is generally fixed to 3.2 W EIRP or 4 W EIRP , according to different countries' regulations. Depending on the size of the tag and on the object on which it is attached, the realized gain of a tag (see Table 1) may span from 3dB (low-loss things) down to -30dB (humans) or even less. Consequently, a UHF link may be established from less than 1m (implantable tags) up to 20m in the best configuration provided that ICs with very high sensitivity are considered in the design (Figure 1). Epidermal UHF tags are expected to be read up to a distance of a few meters.

Table 1 Typical realized gains and read ranges of three families of tags achievable by means of 2014 RFID technology ($P_{\text{chip}} = -22 \text{ dBm}$).

<i>Placement</i>	<i>Realized Gain</i>	<i>Read Range</i>
free-space tag	$0 \div 3 \text{ dB}$	$10 \div 19 \text{ m}$
wearable tag	$-10 \div 0 \text{ dB}$	$4 \div 10 \text{ m}$
epidermal tag	$-20 \div -8 \text{ dB}$	$1 \div 4 \text{ m}$
implanted tag	$< -20 \text{ dB}$	$< 1 \text{ m}$

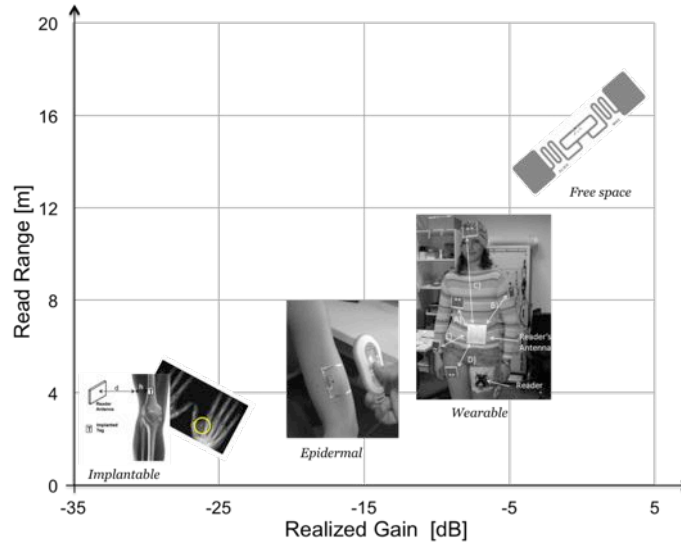


Figure 1. Typical read distances of implantable, epidermal, wearable and free space tag assuming a microchip sensitivity of -22dBm.

3. Radiation Performance of Epidermal Antennas

It is well known that the radiating properties of an antenna are strictly correlated with its physical size [19]. Electrically large antennas generally provide a better gain than smaller ones. For instance, the maximum gain of a straight dipole radiating in free space monotonically increases as function of its electrical length (

Figure 2) and similar curves can be obtained for other layouts such as loops and

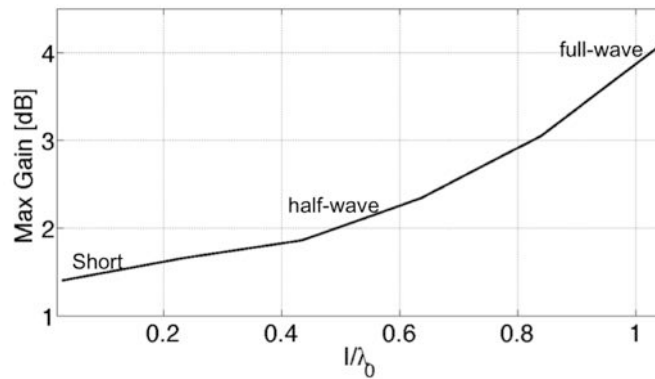


Figure 2. Strip Dipole in free Space: Maximum Gain as a function of the electrical length

slots.

When antennas radiate in the close proximity of a lossy medium like the human body, the radiation efficiency is instead severely degraded because of the high loss of the underlying tissues. Accordingly, the gain-size relationship might be non-trivial and not necessarily monotonic.

In the past, investigation on antennas operating near the interface between air and lossy regions were the topic of extensive theoretical efforts, starting with the famous essay of Sommerfeld in 1909 [20]. Those studies considered simple wire antennas (usually infinitesimal electric or magnetic dipoles) above an infinite lossy half-space and the derived equations and knowledge background had practical concern in a broad variety of applications such as location of buried objects, geophysical prospecting, and over-horizon propagation. Soils and ground generally have a permittivity much lower than the tissues of the human body, while instead a higher conductivity, and the interesting frequencies are rather different than in the UHF-RFID communications.

Among the very few efforts of the RFID community to tackle the challenge of designing passive antennas above lossy medium, the early examples of epidermal transponders are in the form of tattoo-like nested-slot dipoles [15] or dual square loops [33]. The loop shape is traditionally expected, or believed, to outperform dipoles when placed over the body due to the dominant magnetic near field that should be less influenced by the presence of human tissues.

Before introducing possible implementations of epidermal RFID antennas and their applications, it is useful to clarify the role of the geometrical and electrical parameters of dipoles and loops for optimal placement over the skin.

3.1 Efficiency and gain vs. antenna size

Dipole and loop radiators made by a copper trace of $W=1\text{mm}$ width are assumed to be stuck onto a muscle-like box as in

Figure 3 (size $30\text{x}30\text{x}20\text{cm}$, electromagnetic parameters $\epsilon=43$, $\sigma=0.9$ at 870 MHz) through a thin air layer which emulates a thin adhesive membrane. The profiles of maximum gain and radiation efficiency, estimated by the Method of Moments (FEKO solver [21]), are shown in

Figure 4 with respect to the increase of the overall size of the antennas. . More precisely, the length of the dipole and the outer diameter of the loop have been progressively increased up to the effective wavelength $\lambda = \lambda_0 / \sqrt{\epsilon_{\text{eff}}}$ where λ_0 is the free space wavelength and ϵ_{eff} is the effective permittivity evaluated as the average of the permittivity of the body phantom and free space.

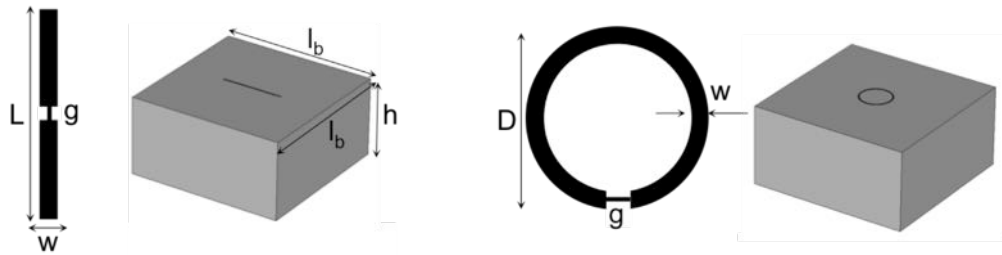


Figure 3. Dipole and Loop radiators over muscle-like box ($l_b=30\text{ cm}$, $h=20\text{cm}$)

Unlike the case of free space radiation, the efficiency of antennas over lossy media exhibits a bell-shaped asymmetrical behavior. After an initial monotonic region with a nearly linear relationship between maximum gain (efficiency) and size, there are peak values, rather similar for the two antennas ($\eta=0.3\%$), occurring for an antenna size of 30mm and 50mm for the loop and the dipole, respectively. In both cases, the significant losses of the tissue induce extremely poor values of radiation gain (-20dB). In the optimal configurations, the length of

the dipole is 0.7λ , while the outer perimeter of the loop is equal to 1.3λ . After the peak value, the maximum gain remains rather stable while instead the radiation efficiency significantly degrades. The peak gains occur along the normal direction

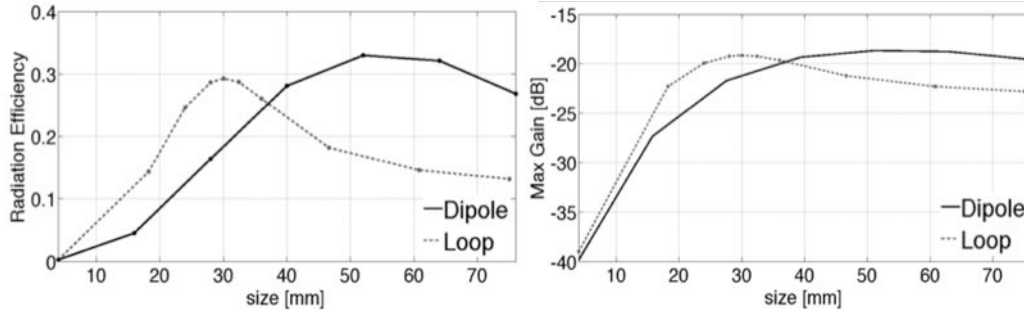


Figure 4. Dipole and Loop Antennas over lossy dense medium: Radiation Efficiency [%] and Maximum Gain at 870 MHz as a function of the maximum size

to the skin, which acts as both an absorber as well as a reflector.

The non-monotonic relationship between the efficiency/gain and physical size of antennas can be explained by considering the presence of two counteracting phenomena. The radiation efficiency can be expressed as the ratio:

$$\eta = \frac{R_R}{R_R + R_O + R_B}$$

where R_R is the radiation resistance of the antenna, R_O is the ohmic loss of the antenna conductor and R_B accounts for the power dissipated by the electromagnetic near field of the antenna into lossy body tissue. The initial rise of the efficiency in Figure 4 is mostly due to the increase of the radiation resistance that is strictly proportional to the overall length of the antenna. However a further enlargement of the antenna will produce more intense power dissipation by the high conductivity of the hosting medium. Thus, enlarging the antenna beyond its optimal size is not only undesirable for epidermal applications demanding small and unobtrusive devices; it even produces a negative impact on radiation properties.

3.2 Gain vs. the trace width

Another geometrical parameter that is involved in the design and fabrication of

epidermal antennas is the width of its conducting traces. Figure 5 shows maximum gain, obtained by simulations, when the copper trace is increased from $W=1\text{mm}$ (as in the previous case) up to 20 mm.

The radiation parameters turned out to be roughly independent on the conductor width, apart from a negligible decrease for the loop. Therefore wider layouts provide the same performance as the narrow ones at the expense of a major invasiveness of the epidermal antennas.

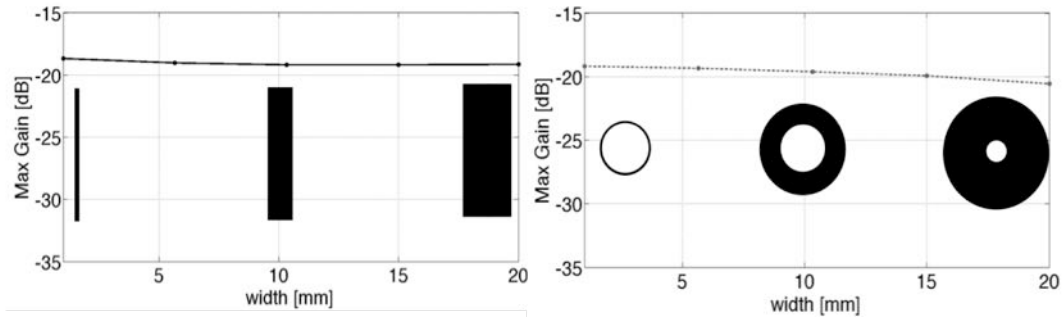


Figure 5. Simulated Maximum Gain at 870 MHz vs the width of the conductor for dipole ($l=50\text{mm}$) and Loop ($r=15\text{mm}$) over lossy medium.

3.3 Radiation performance vs. the trace conductivity

Epidermal devices demand an easy deposition of the conductor traces on thin membranes, and several experiments considered different options than bulk copper, such as inkjet printing or stencil-based techniques which make use of conducting paints and nanoparticle inks [22]. These materials provide superior mechanical performance to the bulk copper, such as flexibility and robustness to cracks, but at the price of a reduced conductivity of one order of magnitude or even more [22].

For antennas radiating in free space, a non-negligible efficiency loss is expected when using bad conductors, while a rather different behavior occurs in the case of epidermal antennas.

Figure 6 shows the efficiency and gain of a dipole of fixed length ($L=50\text{mm}$) and trace thickness $W=1\text{mm}$ when its conductivity is decreased from 10^8 S/m (good conductor) down to 10^2 S/m (bad conductor). There is no visible variation in the radiation performance for $\sigma > 10^4\text{ S/m}$. When further reducing the conductivity

down to 1000 S/m, the gain drops by less than 2 dB. This result is not trivial and it is a consequence of the dominant power losses of the hosting human body that, for epidermal antennas, is much more effective than in case of wearable radiators which are usually much better decoupled from the body.

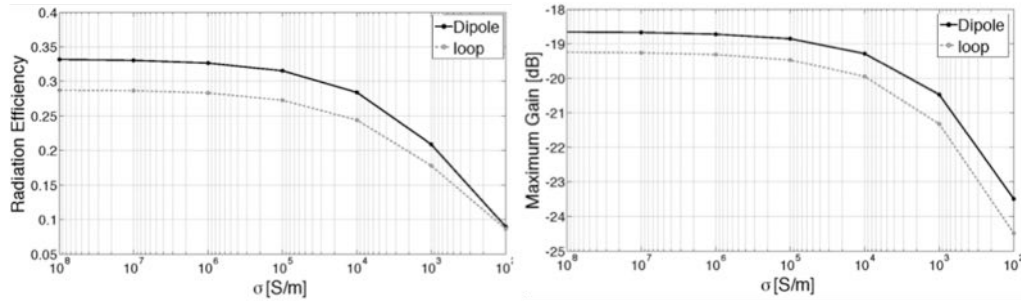


Figure 6. Efficiency and Maximum Gain at 870 MHz vs the finite conductivity of metal conductor.

3.4 Radiation performance vs. the spacing from the skin

Epidermal antennas are stuck onto the skin by ultrathin materials (fractions of millimeters). The membrane could even be functionalized to act as a sensitive material thus enabling the epidermal antenna to act as a sensor. The thickness of the membrane has a remarkable influence on the radiation performance of the antenna since, in case of thick membranes, the electric near field diffused into the epidermis is reduced and, accordingly, the power loss is decreased.

Figure 7 shows the radiation efficiency of a dipole of size ($L=50\text{mm}$, $W=1\text{mm}$, $\sigma=10^8\text{ S/m}$) placed on the same muscle box as before when the skin-dipole gap is increased from $d=0$ (direct contact) up to $600\mu\text{m}$. There is a sharp discontinuity when the separation distance exceeds $d=0.1\text{mm}$ while the efficiency and gain increase is less appreciable for thicker substrates.

To summarize, the close interaction of an antenna (here loops and dipoles) with the lossy human body, and the corresponding strong power loss, induce the following typical phenomena to be accounted for during design and manufacturing:

- i) There is an upper bound in the achievable maximum gain and efficiency, roughly independent of the antenna shape while partly dependent on the thickness of the attaching membrane.
- ii) As a consequence, there is an optimal size of the antenna depending on the particular layout.

- iii) Dipoles and loops provide the same performance. The optimal external size of a loop is however shorter than that of the dipole.
- iv) The quality of the antenna conductor plays a minor role in the radiation performance. Materials with conductivity $\sigma > 10^4$ S/m provide the same results of bulk copper.
- v) The radiation performance sensibly improves when the membrane is thicker than 0.1mm.

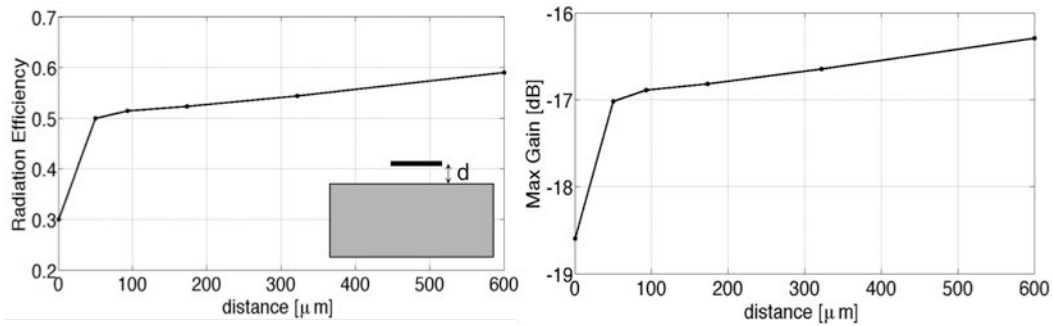


Figure 7. Efficiency and Maximum Gain at 870 MHz as a function of the air gap between the dipole and the muscle box.

4. Performance of Epidermal RFID dual loop-tag

Performances of skin-mounted tags are moreover expected to be quite dependent on the specific region of application due to the high variability of the tissue composition according to different body parts.

In this section a reference UHF tag in the form of dual loop is introduced in order to clarify by means of both simulations and extensive experimentations the dependence of the electromagnetic response on the position over the body and also on the user's body mass. Thanks to the small amount of conductive material and the direct contact with human skin, this tag layout matches the requirements of biocompatibility and low invasiveness of epidermal devices, as well as it is suitable to act as a chemical-electrical transducer of skin conditions.

4.1 Tag Layout

The layout of the epidermal tag consists of a one-wavelength rectangular-loop connected to the RFID microchip through a loop-match impedance transformer [23].

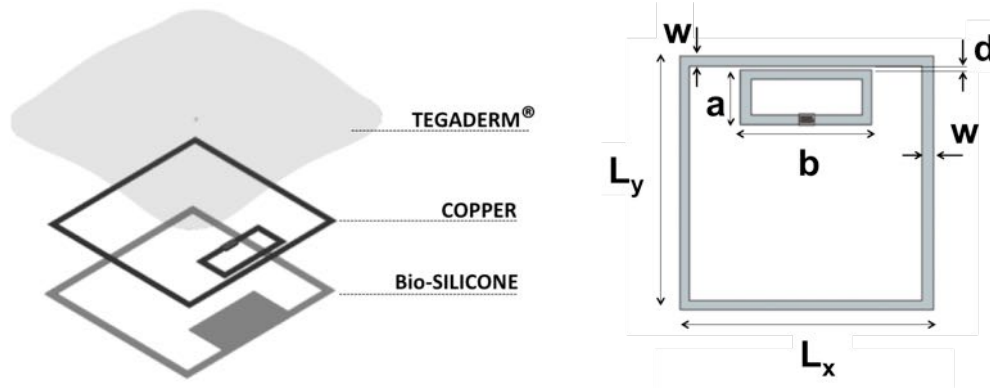


Figure 8. Layout of the epidermal tag. Size [mm]: $L_1 = L_2 = 50$, $w = 2$, $d=0.5$, $a=26$, $b=10$.

A similar geometry has been previously proposed for on-body applications [14]. Unlike the wearable tag, the conductor of the epidermal radiator is insulated from the body by only a thin silicone membrane (thickness $600\mu\text{m}$, $\epsilon = 2.5$, $\sigma=0.005$ S/m) so that the tag is forced to work in very close proximity with the skin. The flexible silicone substrate permits the comfortable application of the tag over any body curvatures and can be carved just around the antenna profile to ensure

physiological skin transpiration (Figure 8). The size of the outer loop is fixed to 5cm x 5cm so that the physical area of the tag is compatible with that of a medical plaster. The internal loop is instead properly sized by numerical simulations (Moment Method throughout FEKO solver [21]) for the optimal impedance tuning within the worldwide UHF-RFID band. The terminals of the inner loop are finally connected to the RFID IC.

The initial design of the tag is performed by exploiting a simplified model of the human body, consisting of stratified planar layers of defined thickness [13], and dielectric properties [24] (see inset in Figure 9). The maximum realized gain of the epidermal tag in this reference configuration (by considering NXP-G2X-TSSOP-8 IC, with $Z_{\text{chip}} = 16 - j148\Omega$, and $P_{\text{chip}} = -15\text{dBm}$) occurs around 940 MHz along the broadside (frontal) direction (Figure 9). The corresponding theoretical read range is hence 2.5m for the considered IC and up to 5.5m in case the state-of-the-art COTS are used ($P_{\text{chip}} = -22.1\text{ dBm}$, [25]).

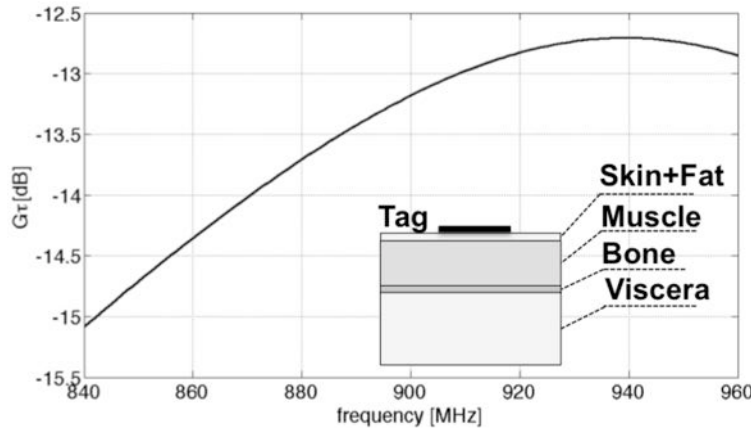


Figure 9. Simulated frequency-dependent realized gain of the epidermal tag over the reference planar model as in [13].

4.2 Prototype and on-skin Performance

Figure 10 shows a prototype of the epidermal tag. It is made of adhesive copper (thickness 35 μm) that was carved by a two-axis digital-controlled cutter. First the loop was transferred over a thick (600 μm) bio-compatible non breathable silicone layer by means of an adhesive transfer tape with the purpose to have a robust substrate which could preserve the integrity of the antenna layout. Then, the membrane was shaped just around the conductors, and the material in excess was

carved out in order to improve transpiration. The resulting gummy loop is finally stuck over a commercial very thin 22 μm transparent adhesive film (TegadermTM). This second membrane is a waterproof and a breathable dressing that is commonly used in clinical practice for the treatment of wounds. The plaster is still partially adhesive, with the copper placed between the two membranes, and it is finally ready for a comfortable and nearly invisible placement over the skin. The ratio between the total area of the conductor and the size of the resulting tag is roughly 20%, with great benefit to skin transpiration. The residual surface of the skin could be moreover used to host other devices such as chemical sensors and even drug delivery mechanisms.

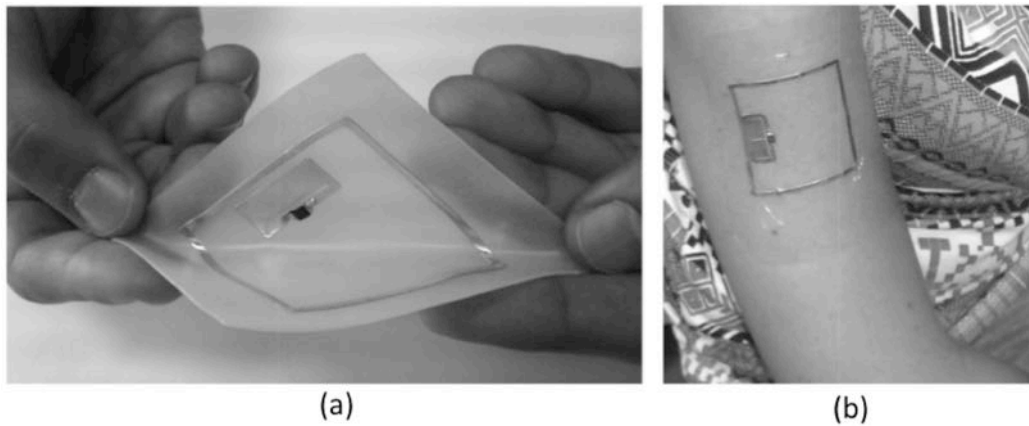


Figure 10. (a) Prototype of the epidermal RFID tag sensor over biocompatible silicone membrane (b) Epidermal RFID tag applied over an arm through TegadermTM fixing.

The performance of the epidermal tag is strictly related to the specific locus of placement over the human body. Figure 11 shows the measured realized gain of the tag placed onto different body districts of a female volunteer such as arm, forearm, abdomen, sternum, hand, neck, and forehead.

The profiles are mutually scaled (due to change in the power absorption) and partially shifted by the effect of impedance detuning. The placement over the leg provides the highest realized gain. In particular, the realized gain is higher than -10dBi at 950MHz and more than -13dBi in the whole UHF RFID band. The worst case was instead the sternum position with a degradation of about 10dB.

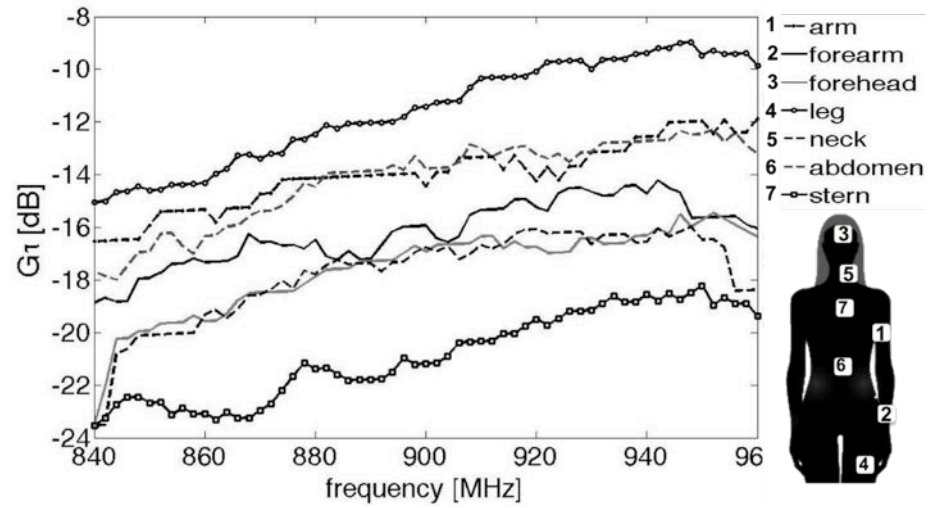


Figure 11. Variability of the measured realized gain of the epidermal tag when attached onto different body districts of a female volunteer.

Tags placed on different subjects suffer from human body variability as visible in Figure 12 where the epidermal tag is attached onto arms, legs and abdomen of three volunteers: a “normal” male, a “muscular” male and a female (height and weight reported in Table 2).

Table 2. Data of the four volunteers for epidermal tag measurements

<i>Volunteer</i>	<i>Height [cm]</i>	<i>Weight [Kg]</i>	<i>Body Mass Index</i>
Female	155	45	18.7
Normal male	174	64	21.4
Muscular male	184	85	25.4

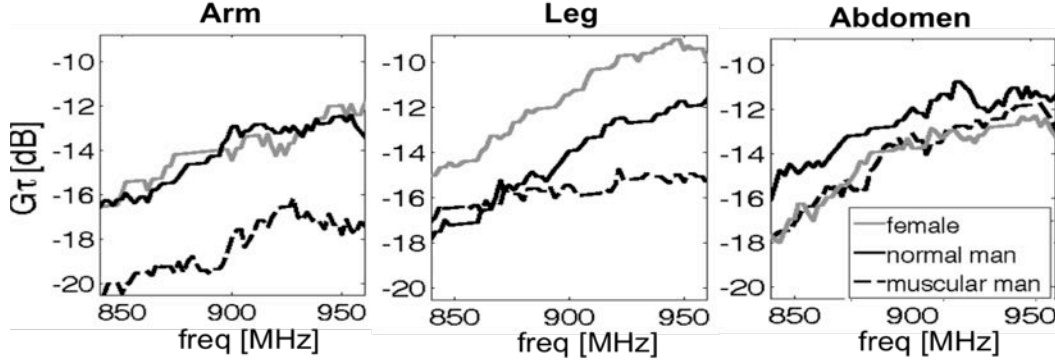


Figure 12. Variability of the measured realized gain of the epidermal tag when it is attached onto corresponding body districts of the three volunteers.

The resulting realized gains are sensibly different in scale and peak position. Tags placed onto normal male and female volunteers exhibit, on average, better performance in comparison with the muscular man. Differences are particularly visible for arm and leg placement while in the case of the abdomen there is no apparent difference between the normal and muscular man since in both cases water-rich tissues dominate. The placement over the leg, for the same reason as above, provides instead the highest gain that, in case of the woman, may approach -9dBi.

4.3 On-skin retuning

Previous experiments demonstrated how the anatomical characteristics of different body regions as well as human body variability (gender, physique) sensibly affect the tag radiation performances. It is hence required to provide the antenna with some post-fabrication and, possibly, post placement retuning capabilities in order to obtain a true communication-reliable epidermal device which is independent of the frequency, of the user's mass and of the specific position

Since the considered tag consists of two loops, it is not possible to achieve tuning by trimming a portion of the conductor length, as typically done with dipoles, since the galvanic continuity of the loop has to be preserved. A viable retuning mechanism relies instead on the form factor of the internal coil. In fact, by analyzing the current distribution over the inner loop (Figure 14(a)), it is apparent that surface currents are more intense in the inner perimeter, so that a perturbation of such a profile is expected to cause a change of the equivalent self-impedance of

the loop and of the mutual inductance between the two coupled loops (recall the equivalent circuit model in [14]), and accordingly the input impedance of the epidermal tag will be modified. A practical way to implement this idea in a controllable manner is to partition the segment of the inner coil, which is closely coupled with the external loop, into some equal-size pre-cut strips (Figure 14 (b)). The strips can be easily removed, even after the placement over the body, to modify the loop current distribution without affecting the tag integrity.

Figure 13 shows the simulated changes of the power transfer coefficient for the epidermal tag when the strongly coupled sub-region of the inner loop ($a=24\text{mm}$, $b=12\text{mm}$) was enlarged and partitioned into six strips of size $20\text{mm} \times 1.9\text{mm}$ and one strip was removed at a time. The tag was again assumed to be placed onto the

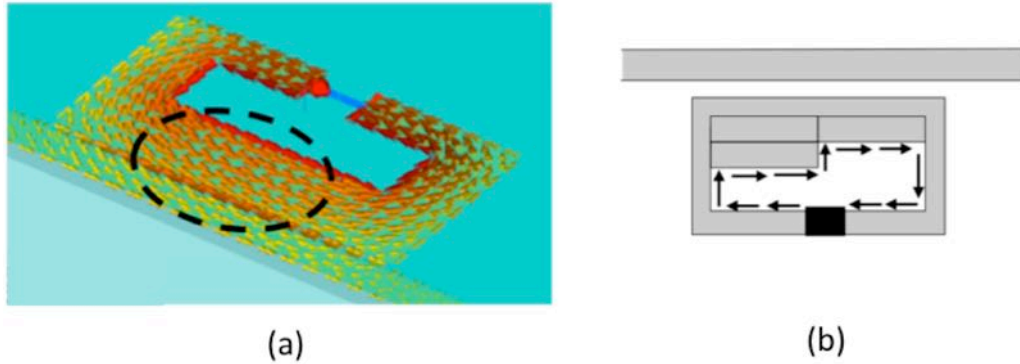


Figure 14. (a) Zoomed view of the simulated current of the feeding loop. (b) The black arrows show how the path of the excitation currents can be modified by removing/adding equal sized strips made of conductor.

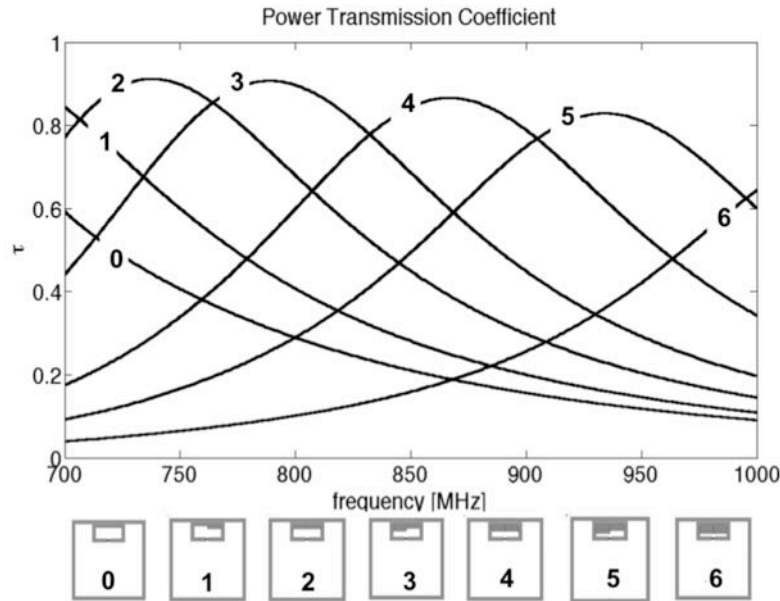


Figure 13. Parametric exploration of the simulated power transmission coefficient of the epidermal tag (placed over the reference layered medium of Figure 9) that is tuned by modifying the size of the feeding inner loop through removal of pre-carved strips of conductors.

layered geometry as in Figure 9. The peak of the power transfer coefficient τ shifts toward a lower frequency, with some improvement in the maximum value.

4.3.1 Examples

Some examples of frequency retuning are given for application of the epidermal tag onto the volunteers. Experiments considered the sensible improvement of performance achievable through the skin retuning in two relevant cases:

1. the realized gain of the tag placed at a given position is initially rather poor;
2. the same tag needs to be used in different RFID band (USA or EU).

The unperturbed tag (e.g. with all the six strips connected) was stuck onto the hip of the female volunteer. The peak of the realized gain occurred at 950 MHz, with a poor maximum value close to -20 dBi (a worse case than those experimented before). An improvement of more than 4 dB was achieved by removing just a single strip and the read distance increased about 1.5 times, as shown in Figure 15.

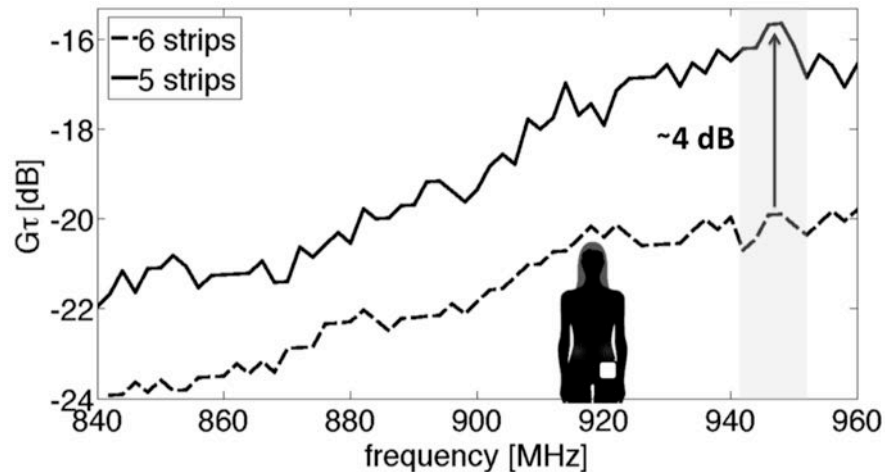


Figure 15. On-skin retuning from US to EU band of the tag placed onto a female hip

Starting from its initial “full” configuration, a tag can be properly tuned to work in any worldwide RFID band by just removing a well-defined number of strips. For example, to have a tag placed on a female arm tuned in the EU band, three strips need to be removed (realized gain at 870MHz equal to -13dBi, Figure 16 while to shift the frequency of operation from Japan to US (realized gain close to -12dBi) for a tag placed on the leg of a normal man the removal of two strips is

(Figure 17) required.

The results of previous experiments may be summarized as in Table 3 to better understand the effectiveness of the on-body retuning. The application of the same tag on different users and on different regions of the body (hip, arm, leg) really benefits at 950 MHz of the retuning (5, 6, 4 strips, respectively) with an overall nearly stable realized gain. The tag with 4 strips is suitable to multiple applications over the hip and arm of the female volunteer at 870MHz and at 900 MHz as well as to the leg of the normal man but at 950MHz. In all cases the read ranges are reasonably similar.

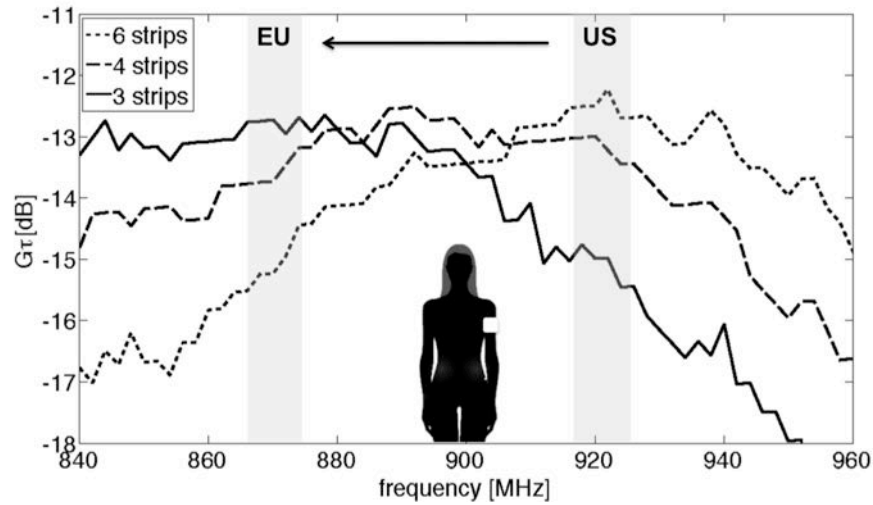


Figure 16. On-skin retuning from US to EU band of the epidermal tag placed onto the arm of the female volunteer.

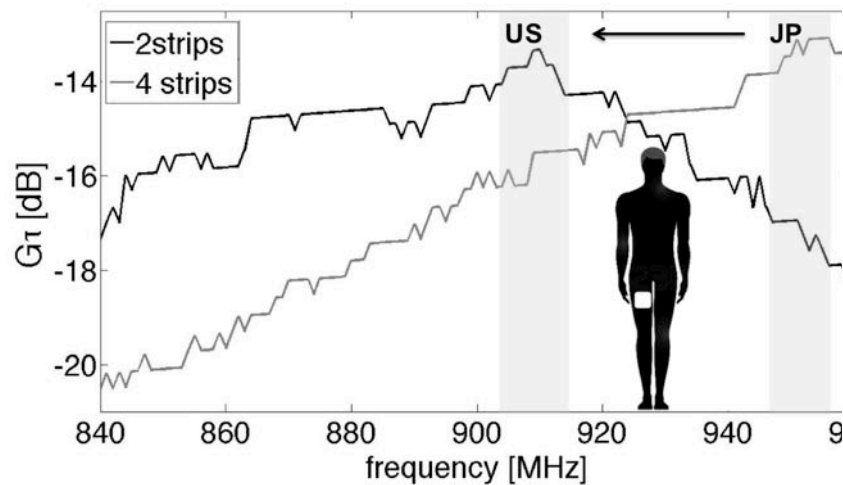


Figure 17. On-skin retuning from US to EU band of the epidermal tag placed onto the leg of the male volunteer.

Table 3. Summary of the strip Number and (Measured Realized Gain) for Some Placement and Frequencies

Placement	870 MHz	900 MHz	950 MHz
Tiny Female, hip	4 (-17 dBi)	4 (-16 dBi)	5 (-16 dBi)
Tiny Female, arm	3 (-13 dBi)	4 (-14 dBi)	6 (-14 dBi)
Normal man, leg	2 (-15 dBi)	2 (-14 dBi)	4 (-15 dBi)

5. Special (functionalized) Epidermal membranes

Epidermal devices must intimately integrate with human skin and enable a fully transparent, non-invasive “on-skin” sampling of bio-parameters. Membranes to be used as substrates for epidermal tags play a crucial role as they represent the interface between the radiators and the human skin. Their mechanical and thermal properties must closely match to the skin itself, such to permit an effective adhesion to the skin surface with minimum constraints on natural processes. From an electromagnetic point of view, the presence of a thin separating layer helps to mitigate the loss from body tissue by concentrating the near field in the low loss region between the antenna and the epidermis (see Section 3.4.).

These materials can act as simple physical means supporting the antenna element or may be instead exploited for sensing purposes in case some of its dielectric and/or geometrical parameters undergo significant variations along with the physio/pathological process under monitoring.

Two classes of unconventional membranes have been proposed as substrates for RFID epidermal tags and sensors, a bioresorbable and transpiring polymeric scaffold, namely *Poli(ϵ -caprolactone)* [26] and an *hydrogel* [27] particularly suited for absorbing and releasing body fluids and drugs and hence for acting as sensitive substrate.

5.1 Scaffold membranes: Poli(ϵ -caprolactone)

Poli(ϵ -caprolactone) (PCL) is a synthetic membrane [26], composed by semicrystalline bioresorbable *poly α -hydroxyester* with a slow degradation rate due to its hydrophobic nature and the high crystallinity degree. This membrane is produced by the electrospinning technique by using PLC granules solved in CHCl_3 and THF:DMF (1:1) solutions. Electrostatic fiber-spinning [28], also

denoted as “electrospinning”, is a straightforward, cost-effective methodology to fabricate non-woven micro and/or nano-fibrous fabrics for several biomedical applications, e.g. scaffolds for tissue engineering or wound dressings. The electrospinning process is activated by applying high voltages between a polymeric solution flowing through a capillary and a collector plate, in order to generate an electrically charged jet, as shown in Figure 18. As the voltage is increased, the electric field intensifies causing a force to build up on the pendant drop of polymer solution at the tip of the needle. This force acts in a direction opposing the surface tension that holds the solution. When the electric field reaches the critical value, the electrostatic force overcomes the surface tension at the tip of the capillary and a continuous charged jet is ejected. When the energized suspension moves away from the needle toward the collector screen, the jet rapidly thins and dries as the solvent evaporates. At the end, the polymer is randomly deposited onto the grounded target forming a dense non-woven membrane that is completely bio-compatible, i.e. free of toxic residues. PCL is moreover flexible and stretchable for a comfortable application over any body curvature and, thanks to its fibrous structure, the natural transpiration of skin is preserved (Figure 18).

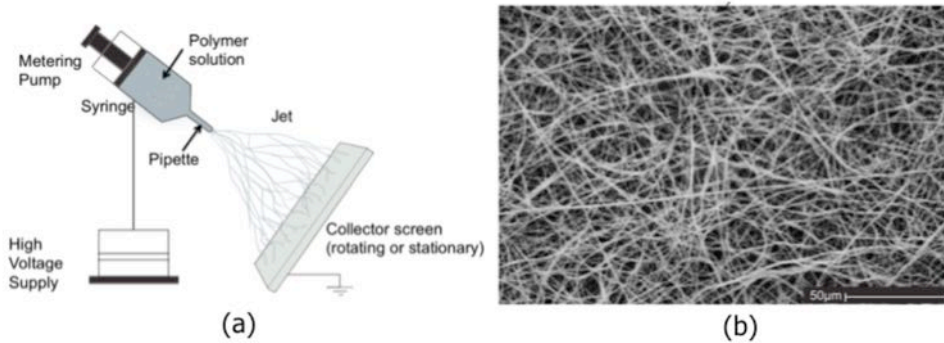


Figure 18. The PCL membrane used as substrate of the epidermal tag. (a) Fabrication scheme by electrospinning. (b) SEM image of the membrane.

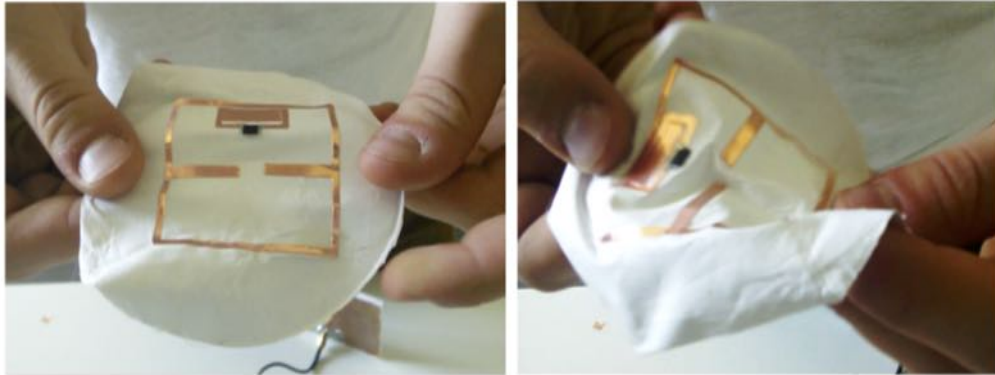


Figure 19. Prototype of the stretched epidermal RFID temperature sensor over PCL membrane.

5.2 Hydrogel membranes

Hydrogel dressings are being extensively investigated for wound treatment as they are able to absorb secretions from exuding wounds, to cool the infected areas, and recover the dehydrated tissues thus creating and maintaining the ideal environment for the wound healing process [27]. These materials can be moreover functionalized by adding doping components to selectively detect biochemical compounds or activate programmable drug release (e.g. antibacterial agents, growth factors). These features, combined with good mechanical properties (flexibility and stretchability), make hydrogels very promising substrates to fabricate RFID-based Smart Plasters.

A hydrogel membrane which has been already experimented for RFID applications [29] is a stretchable substrate made of a polyvinyl alcohol/xyloglucan (PVA/XG). Polyvinyl alcohol is a water-soluble biocompatible synthetic polymer while Xyloglucan is a hemicellulose that occurs in the primary cell wall of every vascular plant. PVA/XG hydrogel membranes is prepared starting from the aqueous solutions of the two polymers, properly mixed at different concentrations. Specific plasticizers can also be added to provide the required flexibility to the membranes, the desired mechanical strength and the bioresorbable degree. Films of different sizes and shapes can be easily produced by natural or forced drying of the mixture (Figure 20).

Similar to conventional hydrogels, the PVA/XG membranes are also able to absorb body fluids (such as wound exudates) and release water and drugs. Their structure hence undergoes swelling and drying processes according to the skin conditions (Figure 21) being able to absorb in the specific case up to 40% of fluid.



Figure 20. PVA/XG membranes under test having different compositions.

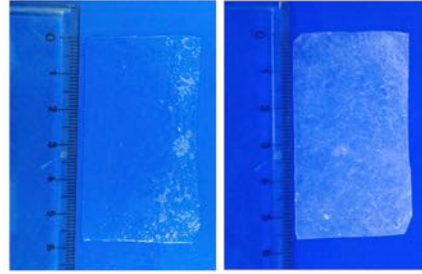


Figure 21. Samples of the fabricated hydrogel membrane. Left) Swollen; Right) Dried

The complex permittivity of the hydrogel membrane in the UHF band is intermediate between that of the PVA powder ($\epsilon = 1.6$, $\sigma = 4.8 \cdot 10^{-3} \text{ S/m}$ [30]) and the much higher permittivity of the absorbed water. Furthermore, great variations are expected during the absorbing and releasing process. A first electromagnetic characterization of such membranes, in both static and dynamical configurations, can be found in [31]. A non-disruptive dielectric probe, comprised of a multi-layer ring resonator, was properly customized with the purpose to correctly measure thin films in variable environmental conditions (Figure 22(a)). The releasing and swelling processes have been then induced by exposing the samples to an electromagnetic liquid phantom resembling the body fluid (saline solution 0.5g/l ($\epsilon_r = 79$, $\sigma = 0.26 \text{ S/m}$)). To enrich the analysis, an additional commercial hydrogel based plaster, *MySkin* [32] was also measured.

In static conditions all the membranes exhibit a low permittivity that is associated with a non-negligible conductivity (Table II) mainly related to the amount of water/fluid absorbed from the environment or residual from the fabrication. The effects are particularly evident in case of the commercial membrane, which contains, as explicitly declared by the producer, a well-defined amount of water to create a wet environment around the wound.

Table 4. Retrieved Dielectric Properties

	M1	M3	M6	M2	M4	M5	MySkin®
ϵ	3.75	4.4	3.7	2.4	2.6	2.5	5.5
$\sigma \text{ [S/m]}$	0.06	0.05	0.08	0.02	0.03	0.02	0.13

During the exposition, the RF response of the membranes significantly changes along with the amount of fluid absorbed in the bulk hydrogel. A remarkable and almost linear variation of permittivity and conductivity (Figure 22(a)) is experienced that sensibly impacts the matching and radiation performance of any RFID epidermal sensors if properly designed and integrated with the membrane.

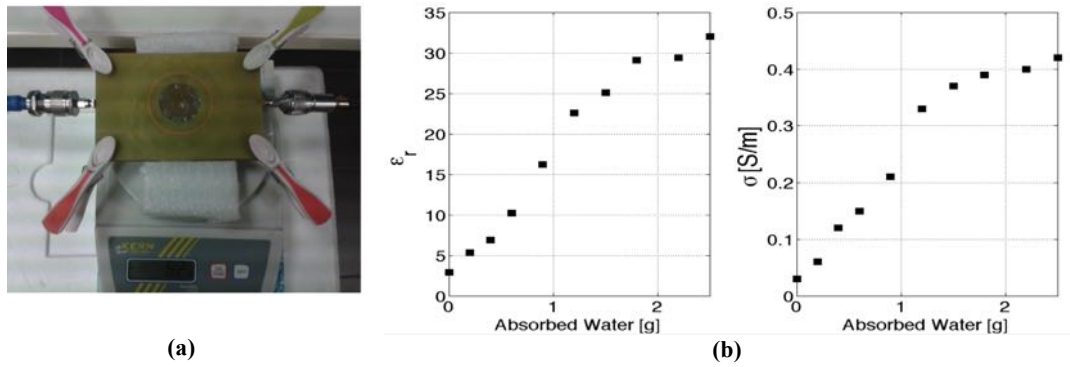


Figure 22. (a) Measurement Setup with a modified version of the ring resonator in [28] with a hole for the dynamic exposition of the sample. (b) Measured dielectric properties of the hydrogel membrane related to the amount of dispersed body fluid.

6. Sensing Applications

Two examples are given of battery-less passive RFID epidermal tags based on the layout described in Section 4 and on the membranes introduced in Section 5. The first one is a thermometer suitable to be used in pathological conditions as well as in sport applications and critical access control [33]. The second one is a sensitive plaster for wound monitoring and healing [29].

6.1 Epidermal RF Thermometer

The temperature sensing mechanism is based on a new family of RFID microchips (EM4325 [34]) equipped with an integrated temperature sensor able to directly provide the measured data in digital form once properly calibrated by means of standard thermocouples [35] (Figure 23(a)). Several independent laboratory tests demonstrated the good accuracy and precision of the RFID sensor, with a standard deviation lower than 0.25°C (Figure 23(b)).

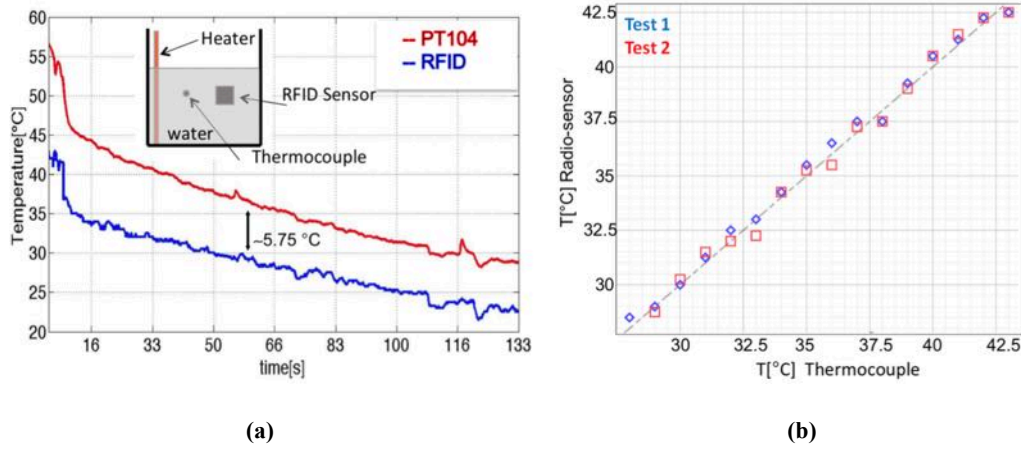


Figure 23. Sensor calibration by a reference thermocouple measurement. (a) Identification of the temperature offset. (b) RFID vs. true (thermocouple) measured temperature profile in further tests by using the calibrated RFID sensor.

The calibrated dual-loop epidermal sensor, integrated with the Poli(ϵ -caprolactone) membrane, was applied to the measurement of body temperature in both rest condition and under physical stress. The sensor was stuck onto the right side of the abdomen (Figure 24) of a male volunteer wearing his usual fitness clothing. A first measurement was conducted for 5min in rest condition, while during the second experimental session the volunteer rode an exercise bike for about 1h.

As expected, at rest the detected temperature was 35°C , that is slightly lower than the core body temperature (about 37°C). During the physical activity instead the temperature followed a slightly cyclic profile due to thermoregulation mechanisms (e.g. sweating changes in skin blood flow) [36]. A substantial agreement with the thermocouple data can be appreciated in both the experiments.

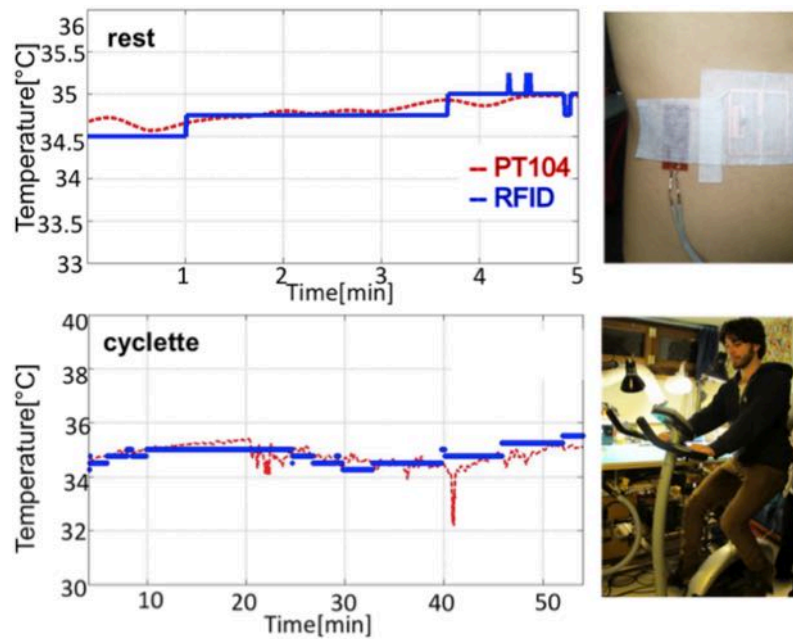


Figure 24 Temperature measurements over the body in rest condition (top) and during physical activity with exercise bike (bottom).

The sensor offers the non-negligible advantage to enable a full wireless interrogation up to 30cm when using a low-power (0.5W EIRP) interrogating device, which can be virtually integrated into mobile phones and handheld devices, or inside the exercise bike itself. By instead using fixed infrastructures, e.g. long-range readers emitting up to 3.2/4 W EIRP, the read distances could increase up to 1m and become compliant with typical access control systems. Passive temperature sensor plasters could indeed open interesting scenarios in the field of health control procedures by sensibly reducing costs and times and by improving their effectiveness and applicability. Great advantages could be offered to the automatic monitoring of people and animals in crowded and transit places (Figure 25), for example in airports, stations, hospitals and rescue camps in which the possibility of epidemic events must be kept under strict control. Furthermore, since temperature is one of the most important health indicators, the passive plasters could be used to unobtrusively monitor the psychological and physical state of operators involved in high-risk operations, such as militaries, firemen and health workers.



Figure 25. Possible setup for the automatic health monitoring of in transit people.

6.2 Smart-plaster for wound healing

A clinical application that could sensibly benefit epidermal electronics is the wound-care, where sensors could be used as diagnostic tools in the healing process [27]. Temperature, pH, and fluid loss could be locally detected by a plaster-sensor and remotely transmitted by using devices either incorporated into or near wound dressings. Furthermore, the possibility to directly modify the clinical therapy, e.g. by modulating the local release of drugs, according to the state of the wound, could open a promising opportunity in the management of diseases such as chronic ulcers, infected acute wounds and large full-thickness burns.

6.2.1 Idea

At the purpose to monitor the loss of fluids or the release of drugs through a body wound, the plaster exploits the absorbing/releasing capabilities of the hydrogel and their effects on tag radiation and matching performances. Indeed, as demonstrated in the previous section, the dielectric properties of the hydrogel strictly depend on the materials composing the membrane and on the amount of absorbed fluid.

With $\Psi(t)$ being the amount of body fluids that are embedded into the hydrogel, it is possible to consider the dependence

$$\Psi(t) \Rightarrow \{\varepsilon_R(\Psi), \sigma(\Psi)\}$$

Accordingly, a change of the fluid percentage will modify the antenna response in terms of input impedance and radar cross section and definitely the activation power of the chip as well as of the backscattered power collected by the reader. By following the formulations in Section 2, different sensing metrics can be easily derived from data measurable by the reader, such as the *realized gain* and the *analog identifier* [9].

The realized gain

$$G_\tau(\theta, \varphi)[\Psi] = \left(\frac{4\pi d}{\lambda}\right)^2 \frac{P_{chip}}{G_R(\theta, \varphi)P_{in}^{to}[\Psi]\eta_P} \quad (1)$$

can be derived by measuring the *turn-on power* $P_{in}^{to}[\Psi]$, while the Analog Identifier AID $[\Psi]$ is a non-dimensional indicator independent on the environment and on the reader-tag mutual position and can be derived by properly combining the forward and backward powers at the turn-on condition as

$$AID[\Psi] = K \frac{P_{chip}}{\sqrt{P_{in}^{to}[\Psi] \cdot P_{bs}^{to}[\Psi]}} \quad (2)$$

The indicators in equations (1) and (2) can be hence used as *data inversion curves* $\xi[\Psi]$ between the measured data and the evolution, $\Psi(t)$, of the fluid loss or delivered to the wound.

6.2.2 Prototype and test

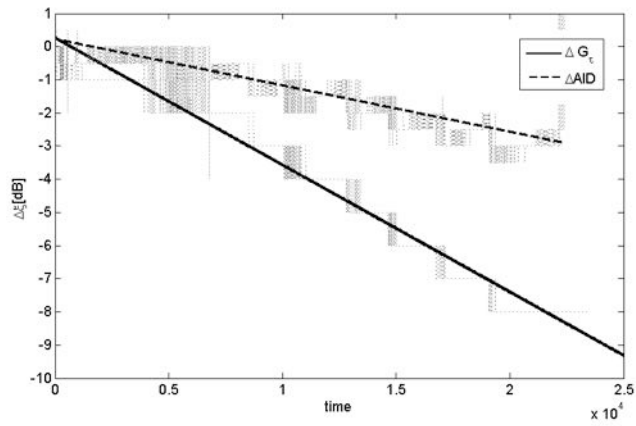
A prototype of the plaster (total weight 2.9g), fabricated on adhesive copper carved by a two-axis digital-controlled cutter, is shown in Figure 26(b). By considering a commercial RFID reader emitting 3.2W EIRP, the tag is expected to be readable in a (0.5÷2.5m) range according to the amount of absorbed fluid.

The sensing capabilities of the RFID plaster has been experimentally characterized by real-time measurements of the realized gain and the analog identifier during both loading (absorption) and recovery processes.

The absorbing process was induced by placing the plaster on a synthetic sponge floating on a plastic box which contains a saline water solution whose electromagnetic parameters resemble those of body fluids. The plaster was continuously interrogated by the reader for an overall measuring time of about 7 hours. As expected, the fluid absorption sensibly impacts the hydrogel features and hence on the tag radiation performances, leading to monotonic and quite linear variation of the sensing curves of $G_r[\Psi]$ and $AID[\Psi]$ with 8dB and 3dB of sensing range respectively (Figure 26 Right).



(a)



(b)

Figure 26 (a) Plaster prototype. (b) Measured absorbing sensing curves at 860MHz (raw and filtered data)

Similar to other hydrogels, the recovery, i.e. the process of releasing the fluid, is in general sensibly slower than the uptake one and it is more dependent on the environmental conditions.

Figure 27 shows the realized gain of the fully loaded plaster after one and two days of recovery, compared with the realized gain of the unloaded membrane. The hydrogel requires more than two days to release all the absorbed fluid. The hysteresis looks negligible in the lower part of the UHF band while it is more evident in the upper part. An insight view on the recovery process is provided in Figure 28 where a partially loaded membrane (amount of absorbed fluid similar to the one produced during body perspiration) has been considered. The profiles are opposite the ones in

Figure 27, demonstrating again the reversibility of the process and the effectiveness of the electromagnetic reaction of the epidermal sensor for smaller amounts of absorbed fluid thanks to the not saturated sensing capabilities in the initial condition. Such observation could open interesting scenarios in the drug delivery area.

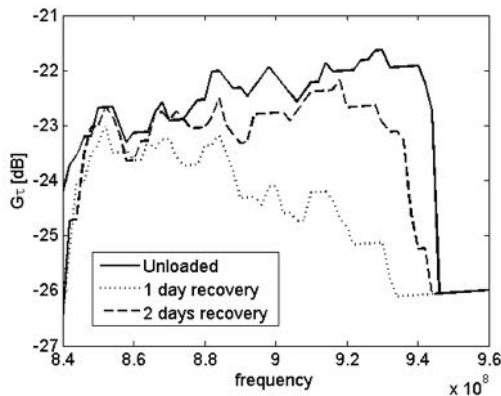


Figure 27. Realized gain of the fully loaded plaster one and two days of recovery with environmental conditions.

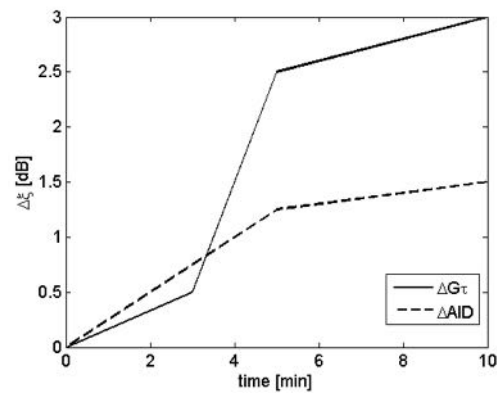


Figure 28 Recovery curves of the electromagnetic response of the RFID plaster when exposed to a small amount of body fluid.

7. Summary and Conclusions

The fertile research on Skin Electronics has paved the way to a novel approach for the continuous assessment of people's health and well-being by pushing the technologies from clothes and personal accessories directly to the human skin. Despite the early studies mostly focused on the high-tech fabrication of engineered thin films with sensor capabilities, there is nowadays an increasing

attention to the powering and communication issues related to the epidermal devices, which are the current bottlenecks for the real spreading of skin-worn technologies.

Numerical investigations on the electromagnetic performance of simple radiators such as dipoles and loops at direct touch with a lossy medium revealed a bell-shape profile of the radiation efficiency with respect to the overall size of the antenna. Depending on the specific layout, there is an optimal size of the antenna (smaller in the case of loop) while the achievable efficiency and, accordingly, the maximum gain have upper bounds roughly independent on the antenna shape.

Inkjet printing or stencil-based methods which make use of conducting paints and nanoparticle inks with low conductivity may be a viable technique for the fabrication of epidermal radiators since the quality of the antenna conductor plays a minor role in the radiation performance.

Unlike shielded wearable tags, epidermal antennas are significantly sensitive to the placement conditions. Simulations and experiments demonstrated that loop-like epidermal tags, insulated from the human skin by only a thin membrane of bio-compatible silicone, provide a realized gain ranging between -17dBi and -9dBi depending on the body district where it is placed and on the body mass of the user. Limbs and arms are the most suitable targets for what concerns communication properties and the epidermal tag may be used for general purpose applications involving just the identification of the user or even wound monitoring and controlled drug delivery. Placement over sternum, forearm and forehead, which are relevant for instance at the purpose of temperature measurement, are instead more critical concerning the RFID link and may hence greatly benefit from on-body retuning.

Substrate materials of epidermal antennas have a crucial role, as they are the interface between the conductor and the epidermis whose local metabolism must be preserved. The radiation performance sensibly improves when the membrane thickness is more than 0.1mm but a trade-off is required for extremely low-profile devices.

First experimentations of epidermal tags fabricated over special membranes demonstrated the feasible application of such devices not only for tracking but also sensing purposes. By providing an epidermal-like tag with an IC embedding digital thermometer, the temperature of the human body was continuously sampled in a wireless and passive mode from a distance up to 1m when using conventional long-range readers, and up to 30cm when using a low-power interrogating device, (e.g. hand-held reader, smartphone). The feasibility of

integrating passive RFID sensor tags into medical hydrogel membranes was also experimentally demonstrated. Indeed, the hydrogel-powered epidermal-tag was revealed to be extremely sensitive to the dynamic exchanges of body fluids at the skin interface thus stimulating innovative solutions for wound care treatment. Conjugate capabilities of both temperature and fluid (e.g. sweat loss) monitoring can be realistically envisaged in the perspective of developing multifunctional RFID Smart plasters.

8. References

- [1] D-H. Kim, N. Lu *et al.*, "Epidermal Electronics", *Science*, Vol. 333, no.12, pp. 838-843, Aug. 2011.
- [2] Yeo, W.H., Kim, Y.S., *et al.* "Multifunctional epidermal electronics printed directly onto the skin", *Advanced Materials*, Vol. 25, Issue 20, pp.2773–2778, May 2013.
- [3] Tao, Hu., *et al.* "Silk-Based Conformal, Adhesive, Edible Food Sensors." *Advanced Materials* 24.8 (2012): 1067-1072.
- [4] Jeong, J.-W., Kim, M. K., Cheng, H., Yeo, W.-H., Huang, X., Liu, Y., Zhang, Y., Huang, Y. and Rogers, J. A. (2014), "Capacitive Epidermal Electronics for Electrically Safe, Long-Term Electrophysiological Measurements". *Advanced Healthcare Materials*, 3: 642–648.
- [5] Rose, D.P.; Ratterman, M.; Griffin, D.K.; Linlin Hou; Kelley- Loughnane, N.; Naik, R.K.; Hagen, J.A.; Papautsky, I.; Heiken- feld, J., "System-level design of an RFID sweat electrolyte sensor patch," *Engineering in Medicine and Biology Society (EMBC), 2014 36th Annual International Conference of the IEEE*, vol., no., pp.4038,4041, 26-30 Aug. 2014
- [6] Kim, Jeonghyun, *et al.* "Epidermal Electronics with Advanced Capabilities in Near-Field Communication", *Small* (2014).
- [7] Dobkin, Daniel M. *The RF in RFID: UHF RFID in Practice*. Newnes, 2012.
- [8] Amendola, S.; Lodato, R.; Manzari, S.; Occhiuzzi, C.; Marrocco, G., "RFID Technology for IoT-Based Personal Health- care in Smart Spaces," *Internet of Things Journal*, IEEE , vol.1, no.2, pp.144,152, April 2014.
- [9] Occhiuzzi, C.; Caizzzone, S.; Marrocco, G., "Passive UHF RFID antennas for sensing applications: Principles, methods, and classifications," *Antennas and Propagation Magazine, IEEE* , vol.55, no.6, pp.14,34, Dec. 2013
- [10] S. Manzari, C .Occhiuzzi, G. Marrocco, "Feasibility of Body-Centric Systems Using Passive Textile RFID Tags," *Antennas and Propagation Magazine, IEEE* , vol.54, no.4, pp.49,62, Aug. 2012.
- [11] Occhiuzzi, C.; Cippitelli, S.; Marrocco, G., "Modeling, Design and Experimentation of Wearable RFID Sensor Tag," *Anten- nas and Propagation, IEEE Transactions on* , vol.58, no.8, pp.2490,2498, Aug. 2010.
- [12] KellomakiT., "On Body performance of Wearable Single Layer RFID Tag", *IEEE Antennas and Wireless Propagation letters*, vol. 11, pp-73-76, 2012.
- [13] Marrocco,G., "RFID Antennas for the UHF Remote Monitoring of Human Subjects," *IEEE Trans. on Antennas Propagat.*, vol.55, no.6, pp.1862,1870, June 2007.
- [14] Tsai, Min-Chuan, *et al.* "Inductively-coupled loop antenna design for UHF RFID on-body applications", *Progress In Elec- tromagnetics Research*, Vol. 143, 315-330, 2013.
- [15] Ziai, M.A.; Batchelor, J.C., "Temporary On-Skin Passive UHF RFID Transfer Tag", *Antennas and Propagation, IEEE Trans- actions on*, Vol.59, no.10, pp.3565,3571, Oct. 2011.
- [16] Rakibet, O.O.; Batchelor, J.C.; Kelly, S.W., "RFID tags as passive enabling technology," *Antennas and Propagation Con- ference (LAPC), 2013 Loughborough* , pp.350,353, 11-12 Nov. 2013.
- [17] Rakibet, O.O.; Rumens, C.V.; Batchelor, J.C.; Holder, S.J., "Epidermal Passive RFID Strain Sensor for Assisted Technologies," *Antennas and Wireless Propagation Letters, IEEE* , vol.13, no., pp.814,817, 2014.
- [18] Makinen, R.M.; Kellomaki, T., "Body Effects on Thin Single- Layer Slot, Self-Complementary, and Wire Antennas," *Antennas and Propagation, IEEE Transactions on* , vol.62, no.1, pp.385,392, Jan. 2014.
- [19] Balanis, Constantine A. *Antenna theory: analysis and design*. John Wiley & Sons, 2012.
- [20] A. Sommerfeld, "The propagation of waves in wireless telegraphy," *Ann. der Phys.*, vol. 28, pp. 665-736; March 1909.
- [21] FEKO Suite 7.0, EM Software and Systems, 2014 [Online]. Available: <http://www.feko.info>.
- [22] V. Sanchez-Romaguera *et al.*, "Towards inkjet-printed low cost passive UHF RFID skin mounted tattoo paper tags based on silver nanoparticle inks", *J. Mater. Chem. C*, 2013, I, 6395-6402.
- [23] H.W.Son and C.S.Tyo, "Design of RFID Tag Antennas Using an Inductively Coupled Feed", *Electronics Letters*, vol. 41, no. 18, pp.994 -996, 2005.

- [24] C. Gabriel, S. Gabriel, "Compilation of the Dielectric Properties of Body Tissues at RF and Microwave Frequencies", Internet document; URL: <http://niremf.ifac.cnr.it/docs/DIELECTRIC/home.html>.
- [25] Monza R6 RFID Tag Chip [Online]. Available: <http://www.impinj.com/products/monza/monza-r6-rfid-tag-chip>.
- [26] Del Gaudio, C., Bianco, A. et al., "Structural characterization and cell response evaluation of electrospun PCL membranes: Micrometric versus submicrometric fibers", *Journal of Biomedical Materials Research Part A*, Vol. 89A, Issue 4, pp.1028–1039, June 2009.
- [27] Tim R. Dargaville, Brooke L. Farrugia, James A. Broadbent, Stephanie Pace, Zee Upton, Nicolas H. Voelcker, "Sensors and imaging for wound healing: A review", *Biosensors and Bioelectronics*, Volume 41, 15 March 2013, Pages 30-42.
- [28] Huang, Zheng-Ming, *et al.* "A review on polymer nanofibers by electrospinning and their applications in nanocomposites." *Composites science and technology*, Vol. 63, Issue 15, pp. 2223–2253, Nov. 2003.
- [29] C.Occhiuzzi, A. Ajovalasitb, M.A.Sabatino, C. Dispenza., G. Marrocco, "RFID Epidermal Sensor including Hydrogel Membranes for Wound Monitoring and Healing", *Proc. Of 9th Annual IEEE International Conference on RFID*, San Diego, CA, April 2015.
- [30] Ebnesajjad S., "Handbook of Biopolymers and Biodegradable Plastics", Elsevier, 1st Edition, 2012.
- [31] S.Amendola, C. Occhiuzzi et al, "Dielectric Characterization of Biocompatible Hydrogels for Application to Epidermal RFID Devices", *Proceedings of European Microwave Conference 2015*, submitted.
- [32] <http://myskin.picsolution.com/en/index.shtml>.
- [33] S. Milici, S.Amendola, A.Bianco and G. Marrocco, "Epidermal RFID Passive Sensor for Body Temperature Measurements", *RFID-Technologies and Applications (RFID-TA), 2012 IEEE International Conference on*, 8-9 September 2014, Tampere (Finland).
- [34] EM4325 IC [Online]. Available: <http://www.emmicroelectronic.com>.
- [35] <https://www.picotech.com/data-logger/pt-104/high-accuracy-temperature-daq>
- [36] Hall, John E., "Guyton and Hall Textbook of Medical Physiology", 12th Edition, Saunders, 2011.